Alternative solvents for lipid extraction and their effect on protein quality in black soldier fly (Hermetia illucens) larvae

Harish Karthikeyan Ravi, Maryline Abert Vian, Yang Tao, Antoine Degrou, Jérôme Costil, Christophe Trespeuch, Farid Chemat

Alternative solvents for lipid extraction and their effect on protein quality in black soldier fly larvae

Harish Karthikeyan Ravi[a], Maryline Abert Vian[a]*, Yang Tao[b], Antoine Degrou[c], Jérôme Costil[c], Christophe Trespeuch[c], Farid Chemat[a]

[a] Avignon Université, INRA, UMR 408, GREEN Extraction Team, F-84000 Avignon, France

[b] College of Food Science and Technology, Nanjing Agricultural University, Nanjing, 210095, China

[c] Mutatec, ZI des Iscles, Chemin des Configues, 13160 Châteaurenard, France

*corresponding author, maryline.vian@univ-avignon.fr

Highlights

- Comparison of alternative solvents for lipid extraction from black soldier fly.
- Lipid extraction was based on theoretical and experimental data.
- 2-methyloxolane (2-MeO) was found to be the ideal green solvent.
- Defatted BSF flour with 2-MeO had relatively better protein quality parameters.

Alternative solvents for lipid extraction and their effect on protein quality in black soldier fly larvae

Harish Karthikeyan Ravi[a], Maryline Abert Vian[a]*, Yang Tao[b], Antoine Degrou[c], Jérôme Costil[c], Christophe Trespeuch[c], Farid Chemat[a]

[a] Avignon Université, INRA, UMR 408, GREEN Extraction Team, F-84000 Avignon, France

[b] College of Food Science and Technology, Nanjing Agricultural University, Nanjing, 210095, China

[c] Mutatec, ZI des Iscles, Chemin des Configues, 13160 Châteaurenard, France

*Corresponding author.

E-mail address: maryline.vian@univ-avignon.fr (Maryline Abert-Vian)

Abstract

Scrutiny of alternative solvents for the extraction of lipid constituents from black soldier fly (BSF) was the main theme of this research. The present investigation compared a wide array of solvents for the extraction of desired components theoretically using tools like Hansen solubility parameters (HSP), conductor-like screening model for real solvents (COSMO-RS) and technical data (ACD labs) with the application of hurdle technology for solvent screening. The ideal solvent selected was 2-methyloxolane (2-MeO) which was employed for conventional and multistage cross-current lipid extraction and the experimental data obtained was compared with that of n-hexane extract. Fatty acid profile, lipid class, bioactivity of the oils were analysed and were in good correlation with the theoretical prediction. The kinetics and diffusion modelling for the extraction system was proposed. The effect of solvent on protein quality parameters like protein dispersibility index, solubility in alkaline solution, urease index in the defatted flour was elucidated. The defatting step had no deleterious effect on the molecular weight distribution of soluble proteins. Overall the study manifested that 2-MeO had better lipid recovery, enhanced bioactivity in the BSF oil, and relatively better protein quality in the defatted flour.

Keywords: Alternative solvents; Black soldier fly; 2-methyloxolane; Lipids; Protein quality.

1. Introduction

In order to feed the growing population which is roughly estimated to touch 9.6 billion by 2050 (FAO, 2017) and alleviate its negative impact on the food supply chain many research units, start-ups, think-tanks and other entities are coming up with innovative, greener alternative solutions to fix the anticipated demand-supply gap. Among the multifarious options being considered to handle the predicaments, utilisation of insects for food and feed applications are gaining significant traction. In particular, *Hermetia illucens* or the Black Soldier Fly larvae (BSFL) belonging to the Diptera order is being contemplated as a promising substitute to replace the conventional protein sources to an extent. Industrial rearing, processing, and valorization of BSFL comes with its own challenges, yet their nature to aggregate the micro, macro-nutrients (Barroso et al., 2017) present in the feeding medium thereby giving proteins, lipids, chitin derivatives, bioactive peptides, and organic manure makes them an attractive candidate for numerous applications.

Hermetia illucens or BSFL for bio-conversion of discarded industrial by-products or side streams, municipal wastes from urban activities have been extensively studied and the economic value it imparts makes it a valuable contender among other solutions recommended. A comprehensive and concise review by Gold et al., 2018 on the decomposition of biowaste types such as human, animal manures, fruits, vegetable wastes, etc. was reviewed recently. Manure management system for laying hens treated with BSFL diminished the manure accumulation by 50% and yielded 42% protein, 35% fat feedstuff is one such example (Sheppard et al., 1994).

Due to the higher lipid concentration (St-Hilaire et al., 2007; Liland et al., 2017), defatting BSFL should be the primary processing step in the downstream valorization of the insect biomass. For the production of protein, fat/oil and chitin, to be used in animal feed, the raw insect materials must undergo a heat treatment process as described in the legislation on animal-by-products (Regulation (EC) No 1069/2009) (EFSA scientific committee., 2015). There is a sharp increase in the number of insect companies foraying into the feed market across continental Europe and North America capitalizing on the new regulation on Novel Foods (EU 2015/2283) passed by the European Parliament. The fortification or replacement of conventional feed with BSFL to augment the protein content has been a time tested idea. The efficacy of BSFL as a feed additive for poultry and a sustainable aquafeed ingredient has been widely advocated (Bondari & Sheppard., 1981; Kroeckel et al., 2012; Vargas-Abundez

et al., 2019). The benefits of BSFL as a feed component is not limited to its protein content and quality, its oil as a potential replacement for soybean oil in Jian Carp diets without any negative effect on growth, feed efficiency in fish fillets was suggested (Li et al., 2016).

In the case of oilseeds, the solvent extraction of oil with n-hexane is preferred as it promotes easier oil recovery and has a narrow boiling point (69 °C). But, n-hexane reacts with free pollutants to form ozone, photo chemicals and is said to affect the neural system when inhaled by humans (Kumar et al., 2017). Though the idea of complete replacement of petrochemical solvents for oil extraction is far-fetched, it is imperative that efforts to reduce the dependency on them and find suitable, economically feasible alternatives for the same must be given due consideration. Several research articles have articulated the effectiveness of green solvents for oil extraction from various biomass. Bio-based solvents for the extraction of oil from rapeseed (Sicaire et al., 2015), the green extraction of lipids from oleaginous yeast biomass (Breil et al., 2016) , the green extraction of *Litsea Cubeba* kernel oil using alternative solvents (Zhuang et al., 2018) are few examples where a green and eco-friendly approach for the extraction of oil was proposed.

The objective of this work was to probe and identify an optimal green solvent from a wide array of solvents including alcohols, ethers, esters and terpenes for defatting the BSFL matrix by combining theoretical and experimental methods. Theoretical data for determining the interactions between the solute and solvent were realized with tools such as Hansen solubility parameters, consequently supported with relatively precise data obtained from conductor-like screening model for real solvent (COSMO-RS) and finally with the application of hurdle technology for decisive selection of suitable solvent based on the absolute theoretical data retrieved. It was within the purview of this study to establish an industrial scale simulation for oil extraction and to develop kinetic modelling for a better understanding of lipid diffusivity in the solvent medium. Furthermore, to elucidate the lipid composition data by identifying the fatty acid profile, lipid class constituents, the bioactivity of BSF oil and compare the effect of solvent on the protein quality parameters in the defatted BSF flour.

2. Materials and methods

2.1. Larvae harvesting conditions

Black Soldier Fly Larvae (BSFL) was provided by a local insect rearing plant based in Avignon region. The larvae were freeze-dried, milled (<1mm), and stored at -18 °C until further analysis. The proximate values of the freeze-dried BSFL were crude nitrogen: 40.27±0.62; crude lipid: 36.41±1.29; ash content: 9.01±0.13; moisture: < 3% (AOAC, 1990)

2.2. Solvents, Standards and Reagents

All solvents for extraction and chromatographic analysis were of analytical grade and purchased from VWR international (Darmstadt, Germany). The solvent 2-methyloxolane also known as 2-methyl tetrahydrofuran (CAS: 96-47-9) was sourced from Honeywell, Sigma-Aldrich Co, St. Louis (MO, USA). Standards: Supelco 37 FAME mix, DL-α-palmitin, glyceryl 1,3-dipalmitate, glyceryl tripalmitate, palmitic acid, phospholipid mixture were purchased from Sigma-Aldrich (USA). Ergosterol, 98% was procured from Acros organics (Germany). Milli-Q water was used for electrophoresis and the protein ladder was sourced from Bio-Rad.

2.3. Extraction

2.3.1. Conventional Soxhlet

The freeze-dried BSFL powder 25 g was taken in a cellulose thimble and subjected to exhaustive Soxhlet extraction for a period of 6 h with 250 mL of n-hexane and 2-MeO solvents respectively. To achieve complete lipid removal the reflux was temporarily stopped every two hours and the sample inside the thimble were mixed thoroughly to facilitate percolation and reduce agglomeration in the matrix. The solvents were collected after 6 – 7 h to establish approximately similar extraction cycles and then evaporated under reduced pressure in a rotavapor. The yield was calculated gravimetrically and extractions were carried out in triplicates.

2.3.2. Multistage cross-current

To mimic the industrial scale oil extraction a multistage cross-current extraction system was set up, wherein three stages of sequential conventional extraction (Fig. 3) was used for maximum oil solubilization in the solvents. The powdered matrix 10 g was mixed with 100 mL solvent for 1 h under constant agitation (150 rpm). Later the solvent was

collected and the residue matrix was subjected to another stage of extraction by infusing 100 mL of fresh solvents with both n-hexane and 2-MeO respectively. This above-mentioned step was repeated again, where the solvent was collected and the residual matrix was extracted again with fresh solvents. The extractions were performed at 55 °C and temperature was maintained using a Huber Pilot system. Therefore in total three stages of conventional extraction was executed and the yield at every stage was noted and the cumulative yield at the end of three stages was compared to conventional Soxhlet extraction results.

2.3.3. Kinetics

The kinetics study comparison to find the solubilization efficacy of both the solvents (n-hexane and 2-MeO) was established by placing 10 g of freeze-dried powder in 100 mL solvent at 55 °C. To understand the lipid extraction with respect to time in both solvents approximately 1 mL of clear solvent was collected from the extraction flask within specific intervals (1,3,5,10,15,20,30,60,90,120,150, and 180 min) and evaporated at 40 °C under nitrogen using a block heater. The yield was calculated and extrapolated to get results for 100g of dry powder.

2.3.4. Diffusion model

During extraction the solvent system was perfectly agitated, therefore, the major mass resistance during extraction was the internal diffusion of lipid within larvae powders (Baümler et al., 2017). In this case, the extraction process can be theorized by the diffusion model based on Fick's second law. Several hypotheses were given prior to simulation (Tao et al., 2017):

a) Larvae powders were regarded as spherical geometry and lipids were initially homogeneously distributed within larvae powders. The radius of the larvae powders was 0.5 mm.

b) The diffusion coefficient of lipid did not change throughout the extraction process. c) Lipid content in larvae particles changed with time and position.

d) No external mass resistance was taken into consideration due to external agitation.

The diffusion equation for spherical geometry is written as (Tao et al., 2017):

$$\frac{\partial C_S}{\partial t} = D_e \left(\frac{1}{x^2} \frac{\partial}{\partial x} \left(x^2 \frac{\partial C_S}{\partial x} \right) \right) \quad (1)$$

where C_s is lipid concentration within larvae particle (g/m^3), De is effective diffusion coefficient for lipid (m^2/s), x is the radial distance in the diffusion direction (m), and t is time (s).

The initial conditions are $C_S = C_{S,0}$ for the solid phase and $C_L = 0$ for the liquid phase. $C_{S,0}$ is the initial concentration of lipid in larvae particles (g/m^3) and C_L is the concentration of lipid in solvent (g/m^3).

The boundary conditions for Eq. 1 are:

$$\left(\frac{\partial C_S}{\partial x}\right)_{x=0} = 0 \tag{2}$$

$$-D_e A\left[\frac{\partial C_S(x,t)}{\partial x}\right]_{x=r} = V\frac{dC_L(t)}{dt} \tag{3}$$

where A is the surface area of larvae particles (m^2), V is the volume of solvent used for extraction (m^3), r is the radius of larvae particles (m).

The "*pdepe*" function in Matlab, R2010a (The MathWorks, Inc., MA, USA) was used to solve the aforementioned parabolic partial differential equation (Tao et al., 2019). To be exact, the original partial differential equation (Eq. 1) was first discretized spatially. After that, the resulting ordinary differential equations were integrated in time and solved by the *pdepe* solver. The D_e value was adjusted iteratively to fit the experimental data, thus minimizing the root mean square error (*RMSE*) between experimental and predicted the content of lipid in larvae particles:

$$RMSE(\mathrm{g/m^3}) = \sqrt{\frac{1}{n}\sum_{i=1}^{n}\left[C_{S,p}(t) - C_{S,e}(t)\right]^2} \tag{4}$$

where $C_{S,e}$ and $C_{S,p}$ is the experimental and predicted values of lipid content in larvae particles (g/m^3), respectively. n is the number of experimental points.

Once the optimized D_e value was obtained, three statistical indicators, including R^2 (coefficient of determination), *RMSE* and absolute average deviation (*AAD*) were calculated using the data about lipid extraction yield to test the predictive accuracy of the diffusion:

$$R^2 = 1 - \frac{\sum_{i=1}^{n}(Y_e - Y_p)^2}{\sum_{i=1}^{n}(Y_e - Y_m)^2} \tag{5}$$

$$RMSE(\mathrm{mg/100g\ DM}) = \sqrt{\frac{1}{n}\sum_{i=1}^{n}\left[Y_p(t) - Y_e(t)\right]^2} \tag{6}$$

$$AAD(\%) = \left[\frac{\sum_{i=1}^{n}(|Y_e - Y_p|)/Y_{S,e}}{n}\right] \times 100 \quad (7)$$

where Y_e, Y_p and Y_m are the experimental, predicted values of lipid extraction yield, respectively (mg/100g DM). Y_m is the average lipid extraction yield (mg/g DM).

Following the numerical simulation results, the distributions of lipid content within larvae powders at different stages of extraction were visualized by programming in Matlab.

2.4. BSFL oil analyses

2.4.1. Fatty acid profile

Fatty acid methyl esters (FAMEs) were prepared from BSF oil samples by acid-catalyzed transmethylation (Breil et al., 2016). Ten to fifteen milligram of oil sample was taken to which 1 mL of methanolic sulfuric acid was added, the mixture was heated in a heating block to facilitate transmethylation and 1.5 mL of 0.9% NaCl solution, and 1 mL of GC-FID grade hexane was added after it reached room temperature. The organic layer was collected and subjected to further analysis. Triheptadecanoin (C17:0; TAG) was used as internal standard and FAME mix was used to calibrate the system. An Agilent (Kyoto, Japan) gas chromatography coupled with a flame ionization detector (GC-FID) system was used to determine the fatty acid profiles of BSF oils. The system was equipped with a BD-EN14103 capillary column with dimensions 30 m × 320 µm × 0.25 µm. The carrier gas (He) velocity was set at 33 $cm.s^{-1}$. The sample injection volume was 2 µL and two washes with n-hexane were executed to avoid carryovers after every sample run. The detection was enabled in split mode (split ratio 1:20), the injection temperature was set at 250 °C. The oven temperature gradient was initially 50 °C for 1 min and then increased at a constant rate of 20 °C/min from 50 °C to 180 °C and then raised from 180 °C to 220 °C at a rate of 2 °C/min. Once it reached 230 °C the temperature was maintained for a period of 10 min and the fatty acids were identified based on retention time and standards used for calibration.

2.4.2. Polar and neutral lipids quantitation

High-performance thin-layer chromatography (ATS 5 automatic TLC sampler, ADC 2 automatic developing chamber, CAMAG 3 TLC scanning densitometer) was used for separation, identification and relative quantitation of the lipid classes of BSF oil extracted with n-hexane and 2-MeO. All stock solutions were prepared in chloroform and 10 mg of sample lipid fraction was used for quantitation. A known volume of lipid extract was loaded

on 20 × 10 cm Silica gel 60 F254 HPTLC plates. Polar lipids were separated with eluent A, a mixture of methyl acetate/isopropanol/chloroform/methanol/KCl (0.25%) in a ratio of 25:25:25:10:9 (v/v/v/v/v). Neutral lipids were eluted with eluent B, a mixture of n-hexane/diethyl ether/glacial acetic acid in a ratio of 70:30:2 (v/v/v). Both plates were allowed to reach a height of 7 cm from the origin, then dried and was dipped in a primuline dye reagent (10 mg of primuline, 160 mL of acetone, 40 mL of distilled water) for better visualization of the lipid classes. Lipid standards were used to identify and quantify the lipid classes in BSF oil.

2.4.3. Total polyphenol content (TPC) and radical scavenging capacity (RSC)

Twenty microliters of appropriate dilutions of the lipid samples or gallic acid (standard) in methanol were taken in a 96-well microplate and 80 µL of 7.5 % Na_2CO_3 solution was added and allowed to equilibrate at room temperature for 10 mins. Rapid addition of 100 µL of 1N Folin-Ciocalteu reagent was completed and absorbance was read at 750 nm for every 5 min over a period of 60 min. Distilled water was used as blank and results were calculated as gallic acid equivalents (GAE).

Similarly, for RSC, 50 µL of samples in the methanolic phase was allowed to react with 0.5 mM methanolic $DPPH^{\bullet}$ radical for 60 mins and the absorbance was measured at 520 nm. Methanol was used as blank, trolox was used for generating the standard curve and results were expressed in trolox equivalent (TE).

2.5. Defatted BSFL flour analyses

2.5.1. Protein molecular weight distribution

Sodium Dodecyl Sulfate-Polyacrylamide Gel Electrophoresis (SDS-PAGE) was used to determine the molecular weight distribution of soluble proteins from BSFL. The proteins were extracted according to Janssen et al., 2017 with few modifications. The dry BSFL powder was placed in citric acid – disodium phosphate buffer (1:10; w/v) and was gently mixed with a magnetic stirrer. After 60 min, the mixture was centrifuged at 9000 rpm for 20 min and the supernatant collected was dialyzed at 18 °C with a dialysis tubing having a cut-off value of 12- 14 kDa and then the dialyzed fraction was subjected to lyophilization to obtain the soluble proteins. The soluble protein 2 mg/ml in milli-Q water was denatured by addition of equal volume of Laemmli sample buffer (65.8mM Tris-HCl at pH 6.8, 26.3% (w/v) glycerol, 2.1% SDS, 0.01% bromophenol blue, 5% 2-mercaptoethanol) at 90 °C for 5

mins and the electrophoresis was run in a Bio-Rad mini-PROTEAN system using TGX pre-cast gels (4-15%).

2.5.2. Protein quantification, dispersibility index, solubility

The nitrogen content in different BSFL solid fractions were analysed by Kjeldahl (Buchi speed digester K-425 system) and the protein content in liquid fractions was calculated by Lowry method with BSA as standard. The defatted BSFL flour protein quality was evaluated according to the quality analyses manual for soybean products in the feed industry (Van Eys et al., 2004) where the protein dispersibility index (PDI), protein solubility in 0.2% potassium hydroxide solution, urease index, and the absorbance at 420 nm were identified.

2.6. Theoretical predictions

For an effective understanding of theoretical data that are generated by tools such as Hansen, COSMO-RS and ACD labs it is essential to establish a local solute solvent database which is specific to the sample chosen for analysis (BSF) and chemical constituents of interest present in them. In this case solvents of different polarity (n-hexane, ethanol, iso-propanol, methyl acetate, ethyl acetate, ethyl lactate, dimethyl carbonate, 2-methyl tetrahydrofuran, cyclopentyl methyl ether, α-pinene, d-limonene, p-cymene) and solutes generally present in the lipid fraction of BSF were chosen after careful literature review. Preliminary parameters was set up with solutes belonging to various classes of the lipid fraction such as free fatty acids (FFA– Lauric Acid), monoglycerides (MAG– Glyceryl 1-laurate), diglycerides (DAG– Glyceryl 1,2-dipalmitate), triglycerides (TAG- Lauric triglyceride), Vitamin E (VE1– α-tocopherol; VE2– γ-tocotrienol), sterols (ST1- β-sitosterol; ST2- Cholesterol) , and pigments (CA1- β-carotene). The solutes were selected based on previously reported data (Liland et al., 2017; Ushakova et al., 2016; Caligiani et al., 2018) on the lipid fraction of BSF.

252 2.6.1. Hansen Solubility Parameters (HSP)

253 HSP helps in understanding the solubility of two compounds, more precisely the
254 miscibility of two components in a medium, it is based on a simple, yet classical principle
255 "like dissolves like" phenomenon. This principle serves as the rule of thumb in characterizing
256 the solute-solvent interactions, theoretically the total cohesive energy density (δ_{total}) is equal
257 to the square root of sum of the energy densities required to overcome atomic dispersion
258 forces (δd^2), molecular polar forces due to dipole moments (δp^2) and hydrogen bonds
259 (loss/gain of proton and exchange of electrons) between molecules (δh^2) and mathematically
260 represented by the following equation:

261 $$\delta_{total} = \sqrt{(\delta d^2 + \delta p^2 + \delta h^2)} \quad (8)$$

262 The magnitude of affinity between solute and solvent is directly proportional to the
263 δ_{total} value, higher the δ_{total} greater the affinity. The relative energy difference (RED) is
264 another parameter that indicates the miscibility of solute in solvents and is calculated:

265 $$RED = \frac{R_a}{R_b} \quad (9)$$

266 where R_a is the distance of a solvent located inside the Hansen solubility sphere and R_b is the
267 radius of the Hansen solubility sphere. The chemical structures and simplified molecular
268 input line entry syntax (SMILES) notations were fabricated using ACD/ChemSketch
269 (Toronto, Canada).

270 2.6.2. Conductor-Like Screening Model for Real Solvents (COSMO-RS)

271 COSMO-RS is used for the calculation of the thermodynamic properties for solvation,
272 without any experimental data. It is the best tool for molecular description and solvent
273 screening based on quantum-chemical approach. The usability of COSMO-RS for
274 determining the relative solubility index $\log_{10}$(x-solub) for sample-specific solutes and
275 solvents has been well documented in our previous work (Ravi et al., 2018). The sheer
276 amount of data generated based on the parameters like σ-surface, σ-profile, σ-potential can be
277 used to predict the compatibility of the solvent for the solubilization of solutes (Fig. 2.). The
278 calculations were executed in a COSMOthermX'17 program (version C30 release 13.01).
279 The standard
280 quantum chemical method triple-valence polarized basis set (TZVP) was used in this study

and 55 °C was the temperature used for the solubility prediction to draw parallels with industrial processing conditions

$$\log_{10}(x_j) = \log_{10}\left[\frac{\exp\left(\mu_j^{pure} - \mu_j^{solvent} - \Delta G_{j,fusion}\right)}{RT}\right] \quad (10)$$

μ_j^{pure}: chemical potential of pure compound j (Joule/mol)

$\mu_j^{solvent}$: the chemical potential of j at infinite dilution (Joule/mol)

ΔG_j, fusion: free energy of fusion of j (Joule/mol)

x_j : solubility of j (g/g solvent).

α-tocopherol (σ-surface) was the solute used in the representative image and for its solubilization in respective solvents (σ -profile, σ-potential) were chosen for theoretical calculations. This process is repeated for all potential solutes, thereby generating the $\log_{10}$(x-solub) values which eventually was compared and tabulated (Table 2.)

2.6.3. Hurdle technology for solvent screening

Application of the hurdle concept has been predominantly used for food preservation, food quality and safety assessment (Khan et al., 2016). It is an excellent decision-making tool that can assist in numerous applications once the factual hurdles are established. For instance, Fig. 1. clearly depicts the impediments that are associated with the solvent selection and how the technical parameters of the solvents are used for solvent screening purposes. A list of candidate solvents are considered and the technical properties such as Log P, boiling point, toxicity index and solvent origin were chosen as appropriate hurdles in this work. These parameters are consolidated (Table 3.) and paves way for taking an informed decision based on the theoretical data available.

3. Results and discussion

3.1. Solvent selection based on theoretical studies

Relative energy difference (RED) is the empirical value that denotes the ability of a solvent to dissolve the solutes of interest present in the sample matrix. The major constituents of BSFL lipid fraction were selected based on literature review, a generalized approach was taken for the solute scrutiny, this way a broader class of compounds can be analysed for their solubility based on Hansen solubility parameters. A representative compound for each class of solutes: lauric acid for fatty acids, glyceryl 1-laurate for monoglycerides, glyceryl 1,2-dipalmitate for diglycerides, lauric triglyceride for triglycerides, α-tocopherol and γ-tocotrienol for vitamin E, cholesterol and β-sitosterol for sterols and finally β-carotene for pigments were selected. It is important to understand that the dietary components of the BSFL heavily influence its chemical composition and is subject to vary drastically based on rearing conditions.

The solvent n-hexane was chosen as a reference and table 1 summarizes the RED scores that were colour coded for easy identification of solvents better than reference. Among the overall class of solvents chosen, ethers and terpenes outperformed the rest. Ultimately, 2-methyloxolane and cyclopentyl methyl ether had the best RED scores for all the solutes considered indicating their theoretical ability to solubilize a wide range of chemical constituents. In case of 2-MeO the RED score ranged between 0.73 for TAG and 1.75 for MAG, similarly, CPME had 0.56 for TAG and 1.76 for MAG as its boundary values. These values symbolise the solvents relative capacity to solubilize the solutes and n-hexane had better theoretical solvation than alcohols and esters collectively. If we look at the data to identify solvents for better solubilization of solutes individually no trend can be found for example α-tocopherol had the best solvation in d-limonene and so did cholesterol which in some cases may not be desirable, hence the model works perfectly for a collectively similar class of compounds (polar or non-polar).

The relative solubility of the lipid contents (Table 2) in different solvents was given by COSMO-RS software which uses quantum calculations from sequential, iterative integration of data generated in the conductor like environment where initially the σ-surface was generated, then σ-profile and σ-potential were used to calculate $\log_{10}$(x_solub) value. The solubilization of solute α-tocopherol as indicated in the example (Fig. 2) was compared with the solvent list wherein the above-mentioned calculations are executed iteratively to

generate the relative value. The ideal solvents had a value of 0 meaning theoretically they were the best solvents for better solubilization of their respective solutes. Again, 2-MeO and CPME proved to be relatively better than other solvents considered. Thus, the collective theoretical result with regard to the solvation power of each solvent for select solutes using Hansen and COSMO-RS determined that 2-MeO and CPME were the best solvents for extraction of lipid-based chemical constituents from BSFL.

Hurdle technology was employed to screen the solvents according to their technical properties (Table 3) such as Log P, boiling point, toxicity index, enthalpy of vaporization, the energy required to evaporate 1 metric ton of solvent, and the nature of solvent (petroleum based, bio-based etc.,). These parameters guide in assessing the ecological footprint associated with usage of solvent for extraction purposes. In the scope of food preservation, hurdle technologies provide a framework for combining a number of preservation techniques for achieving an enhanced level of product safety and stability (Gupta et al., 2012). Similarly, the same concept can be retrieved and applied for solvent screening, the parameters considered were clustered together as hurdles (Fig. 1) and the solvents were assorted based on their classes to observe if there was any trend exhibited by any particular class of solvent. Interestingly, ethers had the upper hand in this scrutiny as well, they were able to surpass all the hurdles showing the versatility and advantages of employing them for extraction. With all parameters and theoretical data considered, CPME and 2-MeO were deduced to be the best suitable solvents and out of the two only 2-MeO is truly a bio-based solvent and produced from lignocellulosic biomass. CPME manufacturing involves the methylation of cyclopentanol or the addition of methanol to readily available cyclopentane (Wanatabe et al., 2007). The mission was to find a green solvent that could potentially replace n-hexane and can be used industrially for oil extraction and 2-methyloxolane met all the criteria put forth and therefore was used for further experimental analyses.

3.2. Solvent performance comparison: yield, fatty acid profile, lipid class

Conventional Soxhlet extraction with n-hexane, 2-MeO recovered 32.51 ± 0.39% and 35.83 ± 1.12% of lipids respectively. The lipid fraction of BSFL comprises of a complex set of substances, the main reason behind such lipid accumulation is that the adult larvae don't feed after the pupal instar ends. This is because of the lack of development of functional mouthparts, rendering them to rely only on the reserves accumulated during larval stages (Gobbi et al., 2013).

The fatty acid profile of oils extracted using n-hexane and 2-MeO were relatively similar (Table 4), lauric acid (C12) was the major fatty acid with 42.29 %, followed by linoleic acid (C18:2n6) with 13.91%, palmitic acid (C16) with 13.83%, oleic acid (C18:1n9) with 11.43%, myristic acid (C14) with 9.36% in decreasing order. These five acids combined made up almost 90% of the fatty acid profile of BSF oils in both cases. The saturated fatty acids were the largest class of fatty acids accounting for 69.13%, followed by polyunsaturated fatty acids responsible for 15.44 % and closely succeeded by monounsaturated fatty acids taking up 14.34%. The data were consistent with previously published results (Liland et al., 2017) with a similar trend of fatty acids being reported. Across all previous research articles that probed the fatty acid profile of BSF, lauric acid was found to be the principal fatty acid with almost 35-40% present in BSF fed average diets, without any extreme feed formulations (Caligiani et al., 2018; Ushakova et al., 2016).

The neutral and polar lipid classes of BSF oils were identified and quantified using HPTLC. Monoglycerides, diglycerides, triglycerides, ergosterol and fatty acid classes were relatively quantified. Free fatty acids were the largest neutral lipid class among the two oils compared, accounting for almost 62% in the 2-MeO lipid fraction and 48% in the n-hexane lipid fraction. In BSF oil extracted with 2-MeO, the sequence was as follows FFA > DAG > ERGO > TAG > MAG, whereas in n-hexane it was FFA > ERGO > DAG > TAG > MAG. The relative quantity of each class is detailed (Fig. 5) with the HPTLC plate of neutral lipids that shows the migration distance of each lipid class. Polar lipids in particular phospholipids were quantified in the 2-MeO BSF oil and were not present in the oil extracted by n-hexane, the solvent polarity plays a major part in extracting polar lipids, sterols, pigments and waxes. This explains the increased oil yield when using 2-MeO as a solvent for defatting as it enhances the overall oil profile by eluting other non-polar constituents present in the matrix. Phosphatidylethanolamine was the primary polar lipid (42%), followed by phosphatidylinositol and phosphatidylcholine present in the 2-MeO BSF oil. This was the first time polar lipids were identified in the lipid fraction of BSF. The absence of polar lipids in n-hexane BSF oil was anticipated. Authors, Ushakova et al., 2016 presented the composition of glycerides in BSFL and attempted to identify other components of the lipid fraction. Dodecanoic ethyl ester, stigmasterol and cholesterol are few of the compounds they quantified, reiterating the importance of understanding lipid prospects of larval biomass and its importance in black soldier fly artificial breeding. Likewise, authors (Liland et al., 2017) vividly elucidated the dietary modulation of BSF with seaweed-enriched media to alter the

lipid profile of BSF, where the total vitamin-E content increased by four folds in the 100% seaweed feed based diet fed to BSF when compared to that of the control. Thus making BSF a unique one-of-a-kind bioreactor like system which aggregates the desired components present in the feed. This particular aspect of BSF as an enriching system is underexplored and can be properly exploited in all field of life sciences and more.

3.3. Oil diffusion kinetics and industrial modelling

While comparing the solvents efficacy to elute lipids from biomass its kinetics aid in understanding the diffusion mechanism with respect to time under predetermined conditions like temperature (55 °C), pressure, agitation (200 rpm). In solid-liquid extraction, the solute of interest in this case oil is readily available and at the very instant that it comes in contact with the solvent it is freely dispersed in the solvent medium. The readily solubilized oil at t = 0-5 min is termed starting accessibility (δXs; g of extract / g of dry matter) signifying the amount of solute solubilized in a limited time frame via the convection of solvent interacting with the surface of the biomass. The oil yield in solvents n-hexane and 2-MeO were plotted against time (Fig. 4a) and the data was extrapolated to 100 g of dry material. The individual oil yield using the solvents n-hexane and 2-MeO indicate the effective diffusivity achieved, exhaustive oil recovery was not accomplished with this setup as it was only meant to give data of oil solubilized as a function of time.

In mass transfer terms, solvent extraction occurs in two stages a) solvent-surface interaction transpires for a short duration, followed by the main mass transfer mechanisms mediated by various b) penetration processes in the solvent-solute system (capillary forces, molecular diffusivity, etc.).

A multistage cross-current system was incorporated to witness the oil recovery efficacy of both the solvents in an industrially scalable system. Three stages of extraction with each stage lasting 1 hour and the solvent replenished at the beginning of every new stage was executed. Incidentally, the cumulative oil yield extracted with this system was precisely the same as the results obtained by conventional Soxhlet system which acknowledges the efficiency and robustness of such system for enhanced oil recovery in a short period of time. After each stage the oil yield was calculated (Fig. 4b) and 2-MeO had relatively higher yield gravimetrically in every stage but when the percentage oil recovery was considered n-hexane (70.2%) had better oil solubilization in stage 1 when compared to that of 2-MeO (66.7%), in subsequent stages 2-MeO exhibited better recovery than n-hexane. The number of stages for

exhaustive lipid recovery can be effectively reduced by supplementing the system with other intensification techniques like ultrasonication, microwave. Ultrasonication in synergy with this system amplified the oil recovery from rapeseed cake (Sicaire A.G. et al., 2016).

3.4. Diffusion modelling and numerical simulation for lipid extraction

The experimental and simulated results of lipid extraction kinetics are illustrated in Fig. 6a. Evidently, the diffusion model provided a satisfactory description of the evolution of lipid yield during extraction, although there were certain divergences in some areas, especial in the early stage of extraction, the overall model was justified for the extraction system. Meanwhile, R^2 values for both cases exceeded 0.96, and *AAD* values were also quite low (Table 5). Accordingly, the diffusion model was qualified to model the extraction process and investigate the mass mechanism using different solvents. The extraction yield at t=0 min was set at 0, so as to enhance the predictive accuracy.

The distributions of lipid content during extraction at 5 and 20 min were visualized in Fig. 6b. There was a relatively high concentration gradient of lipid within larvae powders at the early stage of extraction using n-hexane as a solvent. Along with the increase of extraction time, the lipid concentration gradient decreased. When 2-MeO was used as extraction solvent, the distribution of lipid within larvae powder was more homogenous than that using n-hexane as solvent at the beginning of extraction, probably due to the high extraction rate and fast movement of lipid within the powders.

3.5. Bioactivity of BSF oil

The total polyphenol content (TPC) and radical scavenging capacity (RSC) of the oils were examined (Table 6). BSF oil extracted with 2-MeO had a polyphenol content of 19.03±1.11 mg GAE which was 2.5 times higher than what was present in BSF oil extracted using n-hexane. Comparable results were found in the RSC activity as well, BSF oil (2-MeO) had higher DPPH radical scavenging capacity. The enhanced bioactivity in BSF oil obtained using 2-MeO might facilitate lowered lipid peroxidation at ambient and elevated temperatures and could be used as a functional oil for various dietary supplements in animal feed applications. The vitamin E content contributes to the bioactivity in the lipid fraction, pigments like carotenoids can boost the overall crude oil profile of BSF. The results obtained were compared with refined sunflower oil to establish a reference. Recently, a skincare product with sterilized BSF oil in their formulation was patented (US 2018/0256483 A1). Using alternative solvents to extract oil with enhanced functional properties from insect

biomasses can lead to more innovations and its incorporation in cosmetic and therapeutic formulations.

3.6. Effect of solvent on protein quality in defatted flour

Protein dispersibility index (PDI), is a parameter mostly used to ascertain soybean meal protein quality. It measures the amount of protein dispersed in water after high-speed blending of the biomass. Measuring the PDI for BSF meal (defatted flour) gives a rough idea of protein solubility in water after lipid removal. In this study, the PDI value suggested that 31.6% of the protein in 2-MeO defatted flour and 29.1% of the protein in n-hexane defatted flour was soluble in water indicating a reduced availability of protein in the n-hexane defatted meal.

The presence of non-protein nitrogen in insects specifically in BSFL results in the overestimation of true protein available, therefore a nitrogen-to-protein conversion factor (Kp) value of 4.76 ± 0.09 and 5.6 ± 0.39 was proposed for larvae as such and after protein extraction respectively (Janssen et al., 2017). This might explain the low PDI values in the defatted flours as the crude protein quantitation includes the chitin, glucosamine nitrogen as well, and a Kp value of 6.25 was used for protein assessment. This hypothesis was not probed further as it was out of the scope of this study.

Similarly, protein solubility in 0.2% potassium hydroxide (KOH), urease index (UI), and the absorbance at 420 nm were quantified (Table 7) as these are the generic parameters considered for soybean products in the feed industry. The protein solubility in alkaline conditions for 2-MeO BSF meal was higher than its n-hexane counterpart. As the extraction and analytical conditions were similar the variation in values can be attributed to the nature of the solvent. The crude protein content in 2-MeO BSF and n-hexane meal was 62.16±0.62% and 59.09±0.62% respectively, these results are concurrent, as the lipid recovery was higher in case of 2-MeO thereby concentrating protein content in its corresponding defatted meal. These values combined help determine the protein quality, the state of anti-nutritional factors, and further processing techniques to be employed in soybean meal. The presence of anti-nutritional factors in BSF might depend on the feed substrate, for now very little is known about its presence in BSF reared for feed purposes. Effectively, establishing these values for insect biomass will help potential feed manufacturers relate to the properties of the defatted flour of their respective insect products and compare them to existing industry standards. Insects particularly BSF as a dietary feed for livestock, artic salmon, turbot, crustaceans were

adequately reviewed (Barroso et al., 2013; Makkar et al., 2014; Wang & Shelomi., 2017) projecting the inclusion and infiltration of BSF in feed formulations.

The molecular weight distribution of soluble proteins extracted from 2-MeO defatted BSF flour, n-hexane defatted BSF flour were compared to that of freeze-dried BSF flour (Fig. 7). Almost all proteins belonging to the soluble fractions were within the 25 and 75 kDa range. The most abundant protein band was close to 75 kDa followed by a sharp band next to 50 kDa, these proteins can be enzymes, muscle proteins, exoskeleton proteins or other proteins like melanisation-inhibiting proteins as reported by Yi et al., 2013 for *Tenebrio molitor* larvae. Ideally, since there was no visible change in the protein bands observed by electrophoretic separation it can be assumed that no deleterious effects were imparted during the defatting step at least in the soluble protein fraction. Further protein extraction, fractionation, purification might help throw some light on the elusive protein profile of BSF. The techno-functionality properties of flours and proteins from mealworm and BSFL was compared by Bubler S. et al., 2016 who also found two soluble proteins from BSFL of which the most abundant was identified to have a molecular weight of 80.5 kDa and the other 14.3 kDa. Only one protein was designated in the reviewed section of the UniProt database, it was cecropin-like peptide 1 with accession number: L7VIN3 and molecular mass of 4.84 kDa, supposedly an antimicrobial peptide active against gram-negative bacteria.

The solvent 2-methyloxolane was efficient in lipid recovery and had improved the protein quality in defatted BSF flour while considering it to that of n-hexane defatted flour, making it a better solvent than n-hexane in all technical aspects. Addition of intensification techniques, pre-treatment of the biomass will enhance the extractability and should also be considered to maximise efficiency. Microwave, ultrasound, thermal treatments were effectively used for lipid extraction from yeast (Meullemiestre et al., 2016). A novel Simultaneous Distillation and Extraction Process (SDEP) with alternative terpene solvents for lipid extraction was successfully demonstrated (Tanzi et al., 2013) proving the growing need to find alternative green bio-based solvents to replace toxic petrochemical solvents.

4. Conclusion

Numerous solvents were studied for the extraction of lipid constituents from BSFL biomass. The solvent 2-methyloxolane (2-MeO) was found to be the ideal solvent based on theoretical prediction and experimental results obtained. Extraction kinetics, diffusivity modelling, and industrial simulation for lipid recovery were established. The yield was

significantly higher in 2-MeO BSF oil in conventional as well as the industrial system. Lauric, linoleic, palmitic, oleic, and myristic acids were the major fatty acids. Among the lipid classes, free fatty acids were the major component, phospholipids were identified and quantified in BSF oil (2-MeO) and were absent in BSF oil extracted with n-hexane.

5. Acknowledgements

Harish Karthikeyan Ravi is thankful to Region Sud PACA for the PhD grant.

6. References

AOAC (1990) Official Method of Analysis of the Association of Official Analytical Chemists., AOAC, Arlington, USA

Barroso, F.G., de Haro, C., Sánchez-Muros, M.J., Venegas, E., Martínez-Sánchez, A., Pérez-Bañón, C., 2014. The potential of various insect species for use as food for fish. Aquaculture 422–423, 193–201. https://doi.org/10.1016/j.aquaculture.2013.12.024

Barroso, F.G., Sánchez-Muros, M.-J., Morote, Segura, M., E., Guil, J.-L., Torres, A., Ramos, R., 2017. Insects as food: Enrichment of larvae of Hermetia illucens with omega 3 fatty acids by means of dietary modifications. J. Food Compos. Anal. 62, 8–13. https://doi.org/10.1016/j.jfca.2017.04.008

Baümler, E.R., Carrín, M.E., Carelli, A.A. (2017). Diffusion of tocopherols, phospholipids and sugars during oil extraction from sunflower collets using ethanol as solvent. *Journal of Food Engineering*, 194, 1-8.

Bondari K., Sheppard D.C., 1981. Soldier fly larvae as feed in commercial fish production. Aquaculture, 24, 103-109. https://doi.org/10.1016/0044-8486(81)90047-8

Breil, C., Meullemiestre, A., Vian, M., Chemat, F., 2016. Bio-based solvents for green extraction of lipids from oleaginous yeast biomass for sustainable aviation biofuel. Molecules 21, 1–14. https://doi.org/10.3390/molecules21020196

Bußler, S., Jander, E., Schlüter, O.K., Rawel, H.M., Rumpold, B.A., 2016. Recovery and techno-functionality of flours and proteins from two edible insect species: Meal worm (Tenebrio molitor) and black soldier fly (Hermetia illucens) larvae. Heliyon 2, e00218. https://doi.org/10.1016/j.heliyon.2016.e00218

557 Caligiani, A., Marseglia, A., Sorci, A., Bonzanini, F., Lolli, V., Maistrello, L., Sforza, S.,
558 2018. Influence of the killing method of the black soldier fly on its lipid composition.
559 Food Res. Int. 116, 276–282. https://doi.org/10.1016/j.foodres.2018.08.033

560 EFSA scientific committee, 2015. Risk profile related to production and consumption of
561 insects as food and feed. EFSA J. 13, 4257. https://doi.org/10.2903/j.efsa.2015.4257

562 Gobbi, P., Martínez-Sánchez, A., Rojo, S., 2013. The effects of larval diet on adult life-
563 history traits of the black soldier fly, Hermetia illucens (Diptera: Stratiomyidae). Eur. J.
564 Entomol. 110, 461–468. https://doi.org/10.14411/eje.2013.061

565 Gold, M., Tomberlin, J.K., Diener, S., Zurbrügg, C., Mathys, A., 2018. Decomposition of
566 biowaste macronutrients, microbes, and chemicals in black soldier fly larval treatment:
567 A review. Waste Manag. 82, 302–318. https://doi.org/10.1016/j.wasman.2018.10.022

568 Gupta, S., Kumar, V., Sharma, A., Chatterjee, S., Vaishnav, J., Variyar, P.S., 2012. Hurdle
569 technology for shelf stable minimally processed French beans (Phaseolus vulgaris): A
570 response surface methodology approach. LWT - Food Sci. Technol. 48, 182–189.
571 https://doi.org/10.1016/j.lwt.2012.03.010

572 Janssen, R.H., Lakemond, C.M.M., Fogliano, V., Vincken, J.-P., van den Broek, L.A.M.,
573 2017. Nitrogen-to-Protein Conversion Factors for Three Edible Insects: Tenebrio
574 molitor , Alphitobius diaperinus , and Hermetia illucens . J. Agric. Food Chem. 65,
575 2275–2278. https://doi.org/10.1021/acs.jafc.7b00471

576 Khan, I., Oh, D.-H., Tango, C.N., Lee, B.H., Miskeen, S., 2016. Hurdle technology: A novel
577 approach for enhanced food quality and safety – A review. Food Control 73, 1426–1444.
578 https://doi.org/10.1016/j.foodcont.2016.11.010

579 Kroeckel, S., Harjes, A.G.E., Roth, I., Katz, H., Wuertz, S., Susenbeth, A., Schulz, C., 2012.
580 When a turbot catches a fly: Evaluation of a pre-pupae meal of the Black Soldier Fly
581 (Hermetia illucens) as fish meal substitute - Growth performance and chitin degradation
582 in juvenile turbot (Psetta maxima). Aquaculture 364–365, 345–352.
583 https://doi.org/10.1016/j.aquaculture.2012.08.041

584 Kumar, S.P.J., Prasad, S.R., Kulkarni, K.S., Agarwal, D.K., Banerjee, R., Ramesh, K. V.,
585 2017. Green solvents and technologies for oil extraction from oilseeds. Chem. Cent. J.
586 11, 1–7. https://doi.org/10.1186/s13065-017-0238-8

587 Li, S., Zhou, J., Tian, J., Yu, H., Zhang, B., Ji, H., 2016. Influence of black soldier fly (
588 Hermetia illucens) larvae oil on growth performance, body composition, tissue fatty
589 acid composition and lipid deposition in juvenile Jian carp (Cyprinus carpio var. Jian).
590 Aquaculture 465, 43–52. https://doi.org/10.1016/j.aquaculture.2016.08.020

591 Liland, N.S., Biancarosa, I., Araujo, P., Biemans, D., Bruckner, C.G., Waagbø, R.,
592 Torstensen, B.E., Lock, E.J., 2017. Modulation of nutrient composition of black soldier
593 fly (Hermetia illucens) larvae by feeding seaweed-enriched media. PLoS One 12, 1–23.
594 https://doi.org/10.1371/journal.pone.0183188

595 Liu, P., 2015. The future of food and agriculture: Trends and challenges, Food and
596 Agriculture Organization of the United Nations.

597 Makkar, H.P.S., Tran, G., Heuzé, V., Ankers, P., 2014. State-of-the-art on use of insects as
598 animal feed. Anim. Feed Sci. Technol. 197, 1–33.
599 https://doi.org/10.1016/j.anifeedsci.2014.07.008

600 Meullemiestre, A., Breil, C., Abert-Vian, M., Chemat, F., 2016. Microwave, ultrasound,
601 thermal treatments, and bead milling as intensification techniques for extraction of lipids
602 from oleaginous Yarrowia lipolytica yeast for a biojetfuel application. Bioresour.
603 Technol. 211, 190–199. https://doi.org/10.1016/j.biortech.2016.03.040

604 Ravi, H.K., Breil, C., Vian, M.A., Chemat, F., Venskutonis, P.R., 2018. Biorefining of
605 Bilberry (Vaccinium myrtillus L.) Pomace Using Microwave Hydrodiffusion and
606 Gravity, Ultrasound-Assisted, and Bead-Milling Extraction. ACS Sustain. Chem. Eng. 6,
607 4185–4193. https://doi.org/10.1021/acssuschemeng.7b04592

608 Sangduan C., Sai S., 2018. Skincare products containing Hermetia illucens extract. US
609 2018/0256483 A1.

610 Sheppard, D.C., Newton G.L., Thompson S.A., Savage S., 1994. Avalue added manure
611 management system using the black soldier fly. Bioresour. Technol., 50, 275-279.
612 https://doi.org/10.1016/0960-8524(94)90102-3

613 Sicaire, A.G., Vian, M., Fine, F., Joffre, F., Carré, P., Tostain, S., Chemat, F., 2015.
614 Alternative bio-based solvents for extraction of fat and oils: Solubility prediction, global
615 yield, extraction kinetics, chemical composition and cost of manufacturing. Int. J. Mol.
616 Sci. 16, 8430–8453. https://doi.org/10.3390/ijms16048430

617 St-Hilaire, S., Cranfill, K., McGuire, M.A., Mosley, E.E., Tomberlin, J.K., Newton, L.,
618 Sealey, W., Sheppard, C., Irving, S., 2007. Fish Offal Recycling by the Black Soldier
619 Fly Produces a Foodstuff High in Omega-3 Fatty Acids. J. World Aquac. Soc. 38, 309–
620 313. https://doi.org/10.1111/j.1749-7345.2007.00101.x

621 Tanzi D., C., Abert Vian, M., Chemat, F., 2013. New procedure for extraction of algal lipids
622 from wet biomass: A green clean and scalable process. Bioresour. Technol. 134, 271–
623 275. https://doi.org/10.1016/j.biortech.2013.01.168

624 Tao, Y., Wang, Y., Pan, M., Zhong, S., Wu, Y., Yang, R., Han, Y., Zhou, J. (2017).
625 Combined ANFIS and numerical methods to simulate ultrasound-assisted extraction of
626 phenolics from chokeberry cultivated in China and analysis of phenolic composition.
627 *Separation and Purification Technology*, 178, 178-188.

628 Tao, Y., Han, Y., Liu, W., Peng, L., Wang, Y., Kadam, S., Show, P.L., Ye, X. (2019).
629 Parametric and phenomenological studies about ultrasound-enhanced biosorption of
630 phenolics from fruit pomace extract by waste yeast. *Ultrasonics Sonochemistry*, 52, 193-
631 204.

632 Ushakova, N.A., Kozlova, A.A., Brodskii, E.S., Pavlov, D.S., Kovalenko, A.A., Bastrakov,
633 A.I., 2016. Characteristics of lipid fractions of larvae of the black soldier fly Hermetia
634 illucens. Dokl. Biochem. Biophys. 468, 209–212.
635 https://doi.org/10.1134/s1607672916030145

636 Van Eys, J.E., 2012. Manual of Quality Analyses for Soybean Products in the Feed Industry,
637 2nd edition. U.S. Soybean Export Council.

638 Vargas-Abúndez, A.J., Gasco, L., Truzzi, C., Foddai, M., Giorgini, E., Sanchini, L., Olivotto,
639 I., Randazzo, B., 2018. Insect meal based diets for clownfish: Biometric, histological,
640 spectroscopic, biochemical and molecular implications. Aquaculture 498, 1–11.
641 https://doi.org/10.1016/j.aquaculture.2018.08.018

642 Wang, Y.-S., Shelomi, M., 2017. Review of Black Soldier Fly (Hermetia illucens) as Animal
643 Feed and Human Food. Foods 6, 91. https://doi.org/10.3390/foods6100091

644 Watanabe, K., Yamagiwa, N., Torisawa, Y., 2007. Cyclopentyl methyl ether as a new and
645 alternative process solvent. Org. Process Res. Dev. 11, 251–258.
646 https://doi.org/10.1021/op0680136

647 Yi, L., Lakemond, C.M.M., Sagis, L.M.C., Eisner-Schadler, V., Huis, A. Van, Boekel,
648 M.A.J.S.V., 2013. Extraction and characterisation of protein fractions from five insect
649 species. Food Chem. 141, 3341–3348. https://doi.org/10.1016/j.foodchem.2013.05.115

650 Zhuang, X., Zhang, Z., Wang, Y., Li, Y., 2018. The effect of alternative solvents to n-hexane
651 on the green extraction of *Litsea cubeba* kernel oils as new oil sources. Ind. Crops Prod.
652 126, 340–346. https://doi.org/10.1016/j.indcrop.2018.10.004

Figure caption.

Figure 1. Application of hurdle technology for solvent screening.

Figure 2. Representative image for theoretical solubility prediction using COSMO-RS.

Figure 3. Graphical representation of the design of experiment.

Figure 4. a) BSF oil extraction kinetic curve **b)** Oil yield in multistage cross-current extraction system.

Figure 5. a) Relative content of neutral lipids in BSF oil **b)** Relative content of polar lipids in BSF oil **c)** HPTLC plate of neutral lipids.

Figure 6. a) Experimental versus predicted values of lipid extraction yields. ●: n-hexane; ●: 2-MeO; The solid lines represent the diffusion model. **b)** Visuals of lipid content distribution within larvae powders during extraction using the numerical simulation results.

Figure 7. Molecular weight distribution (kDa) of soluble proteins of freeze dried and defatted flour, FDBSF – Freeze Dried Black Soldier Fly; HR – n-hexane residue; 2-MeO – 2-methyloxolane residue.

Table 1. Solvent selection based on RED scores of Hansen Solubility parameters

Solute	FFA	MAG	DAG	TAG	VE1	VE2	ST1	ST2	CA1
Solvent	Relative Energy Difference : RED score								
n-hexane	2.24	3.21	2	1.24	1.4	2.03	1.5	1.6	1.49
Ethanol	3.22	2.23	3.42	4.39	4.39	4.25	4.42	4.28	4.9
Iso-propanol	2.3	1.34	2.47	3.48	3.44	3.33	3.49	3.35	3.97
Methyl acetate	0.89	1.09	1.15	1.69	1.88	2.07	1.91	1.79	2.41
Ethyl acetate	0.42	1.05	0.64	1.28	1.42	1.62	1.47	1.35	1.98
Ethyl lactate	1.55	0.65	1.81	2.69	2.73	2.69	2.76	2.62	3.26
DMC	1.34	0.97	1.62	2.29	2.44	2.54	2.47	2.34	2.97
2-MeO	0.89	1.75	0.98	0.73	0.89	1.09	0.84	0.75	1.27
CPME	0.83	1.76	0.85	0.56	0.73	1.02	0.71	0.61	1.17
α-pinene	1.56	2.55	1.35	0.46	0.49	1.11	0.57	0.68	0.67
d-limonene	1.07	2	0.92	0.55	0.24	0.48	0.23	0.13	0.7
p-cymene	1.45	2.39	1.34	0.53	0.43	0.72	0.29	0.38	0.42

Gray - Reference solvent; Green - Equivalent or better than reference; Red - Worse than reference

*FFA- Lauric acid; MAG- Glyceryl 1-laurate; DAG- Glyceryl 1,2-dipalmitate; TAG- Lauric triglyceride; VE1- α-tocopherol; VE2- γ-tocotrienol; ST1- β-sitosterol; ST2- cholesterol; CA1- β-carotene

**DMC- Dimethyl carbonate; 2-MeO- 2-methyloxolane; CPME- Cyclo pentyl methyl ether

Table 2. Solvent selection based on the solubility index log10(x_solub) of COSMO-RS

Solute*	FFA	MAG	DAG	TAG	VE1	VE2	ST1	ST2	CA1
Solvent**	Solubility index : $\log_{10}$(x-solub)								
n-hexane	-1.0307	-2.1617	-0.6419	-0.1963	0	-0.345	-0.4479	-0.1823	0
Ethanol	0	0	-0.5865	-1.0797	-0.8543	-0.0836	-0.5312	-0.7166	-1.7267
Iso-propanol	0	0	-0.1874	-0.7162	-0.5073	0	-0.2727	-0.4068	-1.3477
Methyl acetate	0	0	0	-0.0394	0	0	-0.2694	-0.255	0
Ethyl acetate	0	0	0	0	0	0	-0.0307	0	0
Ethyl lactate	0	0	0	0	0	0	-0.0798	-0.0743	-0.1278
DMC	-0.2469	-0.3211	-0.7839	-0.6539	-0.5882	0	-0.8265	-0.8554	-0.5794
2-MO	0	0	0	0	0	0	0	0	0
CPME	0	0	0	0	0	0	0	0	0
α-pinene	-0.9093	-1.9464	-0.5993	-0.1173	-0.0119	-0.2729	-0.4623	-0.232	0
d-limonene	-0.7317	-1.6106	-0.3792	0	0	-0.0869	-0.3972	-0.1979	0
p-cymene	-0.7266	-1.5291	-0.4172	0	0	-0.0739	-0.4638	-0.2939	0

Gray - Reference solvent; Green - Ideal solvent; Yellow - Equivalent or better than reference; Red - Worse than reference
*FFA- Lauric acid; MAG- Glyceryl 1-laurate; DAG- Glyceryl 1,2-dipalmitate; TAG- Lauric triglyceride; VE1- α-tocopherol; VE2- γ-tocotrienol; ST1- β-sitosterol; ST2- cholesterol; CA1- β-carotene
**DMC- Dimethyl carbonate; 2-MO- 2-methyloxolane; CPME- Cyclopentyl methyl ether

Table 3. Technical parameters for solvent screening

Solvents / Parameters	Log P	Boiling point	Toxicity index	Energy required to evaporate 1 metric ton of solvent (kW.h)	Enthalpy of vaporization [$\Delta_{vap}H(T_{bp})$]; kJ/mol
n-hexane	3.9	68	6	120.1	28.85
Ethanol	-0.2	78.37	5	268.6	38.56
Iso-propanol	0.2	82.5	5	225.8	39.85
Methyl acetate	0.2	57.1	5	130.8	30.32
Ethyl acetate	0.7	77.1	5	128.7	31.94
Ethyl lactate	-0.2	154	5	171.0	45.57
DMC	0.2	90	5	134.8	33.05
2-MeO	0.8	80.2	4	126.1	30.74
CPME	1.4	106	4	132.4	33.00
α-pinene	4.4	155	4	142.5	37.83
d-limonene	4.4	176	5	153.8	37.83
p-cymene	4.0	177	5	155.8	39.34

Green – Good score; Yellow – Average score; Red – Poor score (relative comparison).
DMC- Dimethyl carbonate; 2-MO- 2-methyloxolane; CPME- Cyclopentyl methyl ether.

-

Table 4. Relative percentage of fatty acid profiles of BSF oil

Fatty acids	n-hexane (%)	2-MeO (%)
C10	1.02 ± 0.01	1.02 ± 0.00
C12	42.27 ± 0.13	42.29 ± 0.18
C14	9.41 ± 0.01	9.36 ± 0.01
C14:1	0.19 ± 0.01	0.18 ± 0.00
C15	0.18 ± 0.01	0.18 ± 0.00
C15:1	0.06 ± 0.01	0.06 ± 0.00
C16	13.91 ± 0.05	13.83 ± 0.00
C16:1	2.73 ± 0.02	2.67 ± 0.00
C18	2.28 ± 0.01	2.23 ± 0.01
C18:1n9	11.84 ± 0.05	11.43 ± 0.12
C18:2 n6 trans	14.29 ± 0.09	13.91 ± 0.03
C18:3n3	1.41 ± 0.01	1.37 ± 0.01
C20	0.16 ± 0.01	0.16 ± 0.00
C22	0.06 ± 0.00	0.06 ± 0.00
C22:2 n6	0.17 ± 0.01	0.16 ± 0.00
Σ SFAs	69.29	69.13
Σ MUFAs	14.82	14.34
Σ PUFAs	15.87	15.44
Others	0.02	1.09

SFA - Saturated Fatty acids
MUFA - Mono Unsaturated Fatty Acids
PUFA - Poly Unsaturated Fatty Acids

Table 5. Effective diffusion coefficients of lipids at different extraction conditions and accuracy of the diffusion model

Solvent	De (m^2/s)	R^2	RMSE (mg/100g DM)	AAD (%)
n-hexane	2.17×10^{-9}	0.99	0.438	3.27
2-MeO	6.67×10^{-10}	0.97	1.013	4.75

*D*e – Effective diffusion coefficient for lipid; R^2 – Coefficient of determination; RMSE – Root Mean Square Error; AAD – Absolute Average Deviation

Table 6. Total Polyphenol Content and Radical Scavenging Capacity of BSF oil

Description	TPC (mg GAE/g of oil)	RSC (mg TE/g of oil)
Refined sunflower oil (reference)	3.60 ± 0.09	0.79 ± 0.17
BSF oil (n-hexane)	7.42 ± 0.51	0.41 ± 0.03
BSF oil (2-MeO)	19.03 ± 1.11	5.42 ± 0.76

GAE - Gallic Acid Equivalent; TE - Trolox Equivalent.

Table 7. Protein quality evaluation of defatted BSF flour

Protein quality parameters	Defatted BSF (n-hexane)	Defatted BSF (2-MeO)
Crude protein; %	59.09 ± 0.62	62.16 ± 0.62
PDI; %	29.09	31.55
PS - KOH; %	78.29	80.6
UI; Δ pH units	0.13	0.15
Abs @ 420nm	0.063	0.071

PDI -Protein Dispersibility Index; PS - Protein solubility in 0.2 % KOH.

UI - Urease Index; Abs - Absorbance at 420 nm.

Figure 1.

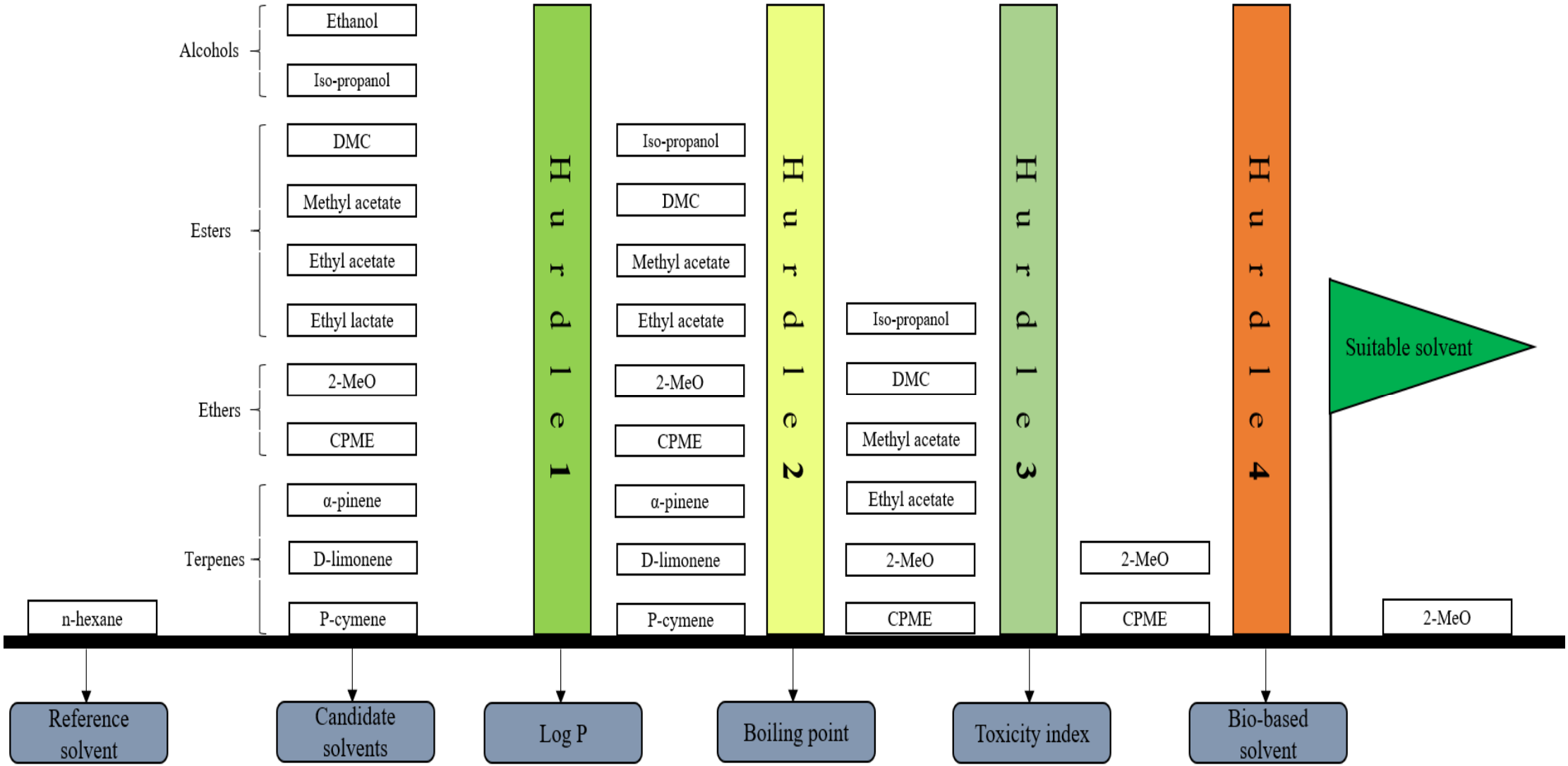
Alcohols
Ethanol
Iso-propanol
Esters
DMC
Methyl acetate
Ethyl acetate
Ethyl lactate
Ethers
2-MeO
CPME
Terpenes
α-pinene
D-limonene
P-cymene
n-hexane
Hurdle 1
Iso-propanol
DMC
Methyl acetate
Ethyl acetate
2-MeO
CPME
α-pinene
D-limonene
P-cymene
Hurdle 2
Iso-propanol
DMC
Methyl acetate
Ethyl acetate
2-MeO
CPME
Hurdle 3
2-MeO
CPME
Hurdle 4
Suitable solvent
2-MeO
Reference solvent
Candidate solvents
Log P
Boiling point
Toxicity index
Bio-based solvent

Figure 2.

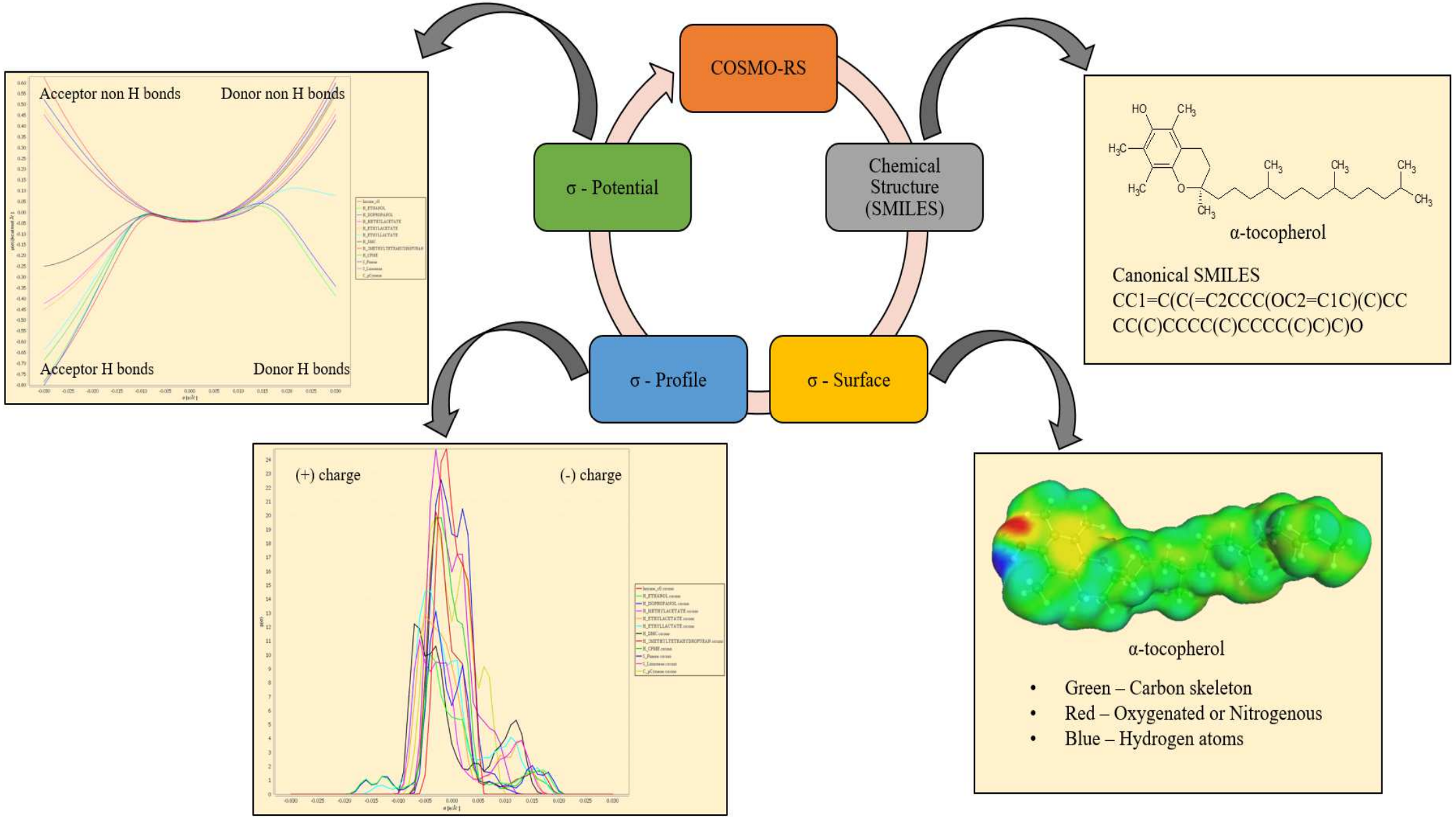
COSMO-RS
σ - Potential
Chemical Structure (SMILES)
σ - Profile
σ - Surface
Acceptor non H bonds
Donor non H bonds
Acceptor H bonds
Donor H bonds
(+) charge
(-) charge
α-tocopherol
Canonical SMILES
CC1=C(C(=C2CCC(OC2=C1C)(C)CCCC(C)CCCC(C)CCCC(C)C)C)O
α-tocopherol
Green – Carbon skeleton
Red – Oxygenated or Nitrogenous
Blue – Hydrogen atoms

Figure 3.

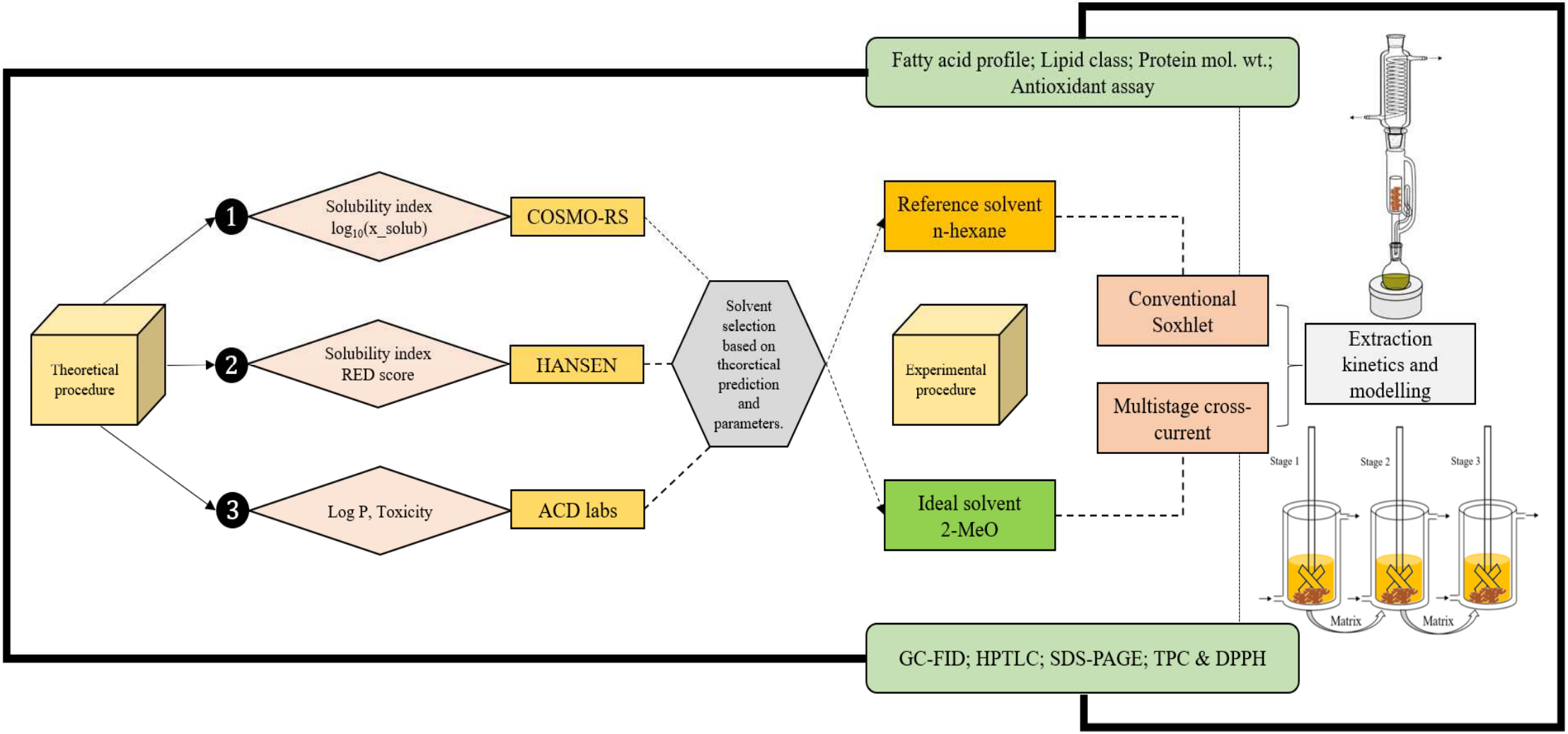
Fatty acid profile; Lipid class; Protein mol. wt.; Antioxidant assay
Theoretical procedure
1
Solubility index log_{10}(x_solub)
COSMO-RS
2
Solubility index RED score
HANSEN
3
Log P, Toxicity
ACD labs
Solvent selection based on theoretical prediction and parameters.
Reference solvent n-hexane
Experimental procedure
Ideal solvent 2-MeO
Conventional Soxhlet
Multistage cross-current
Extraction kinetics and modelling
Stage 1
Stage 2
Stage 3
Matrix
Matrix
GC-FID; HPTLC; SDS-PAGE; TPC & DPPH

Figure 4.

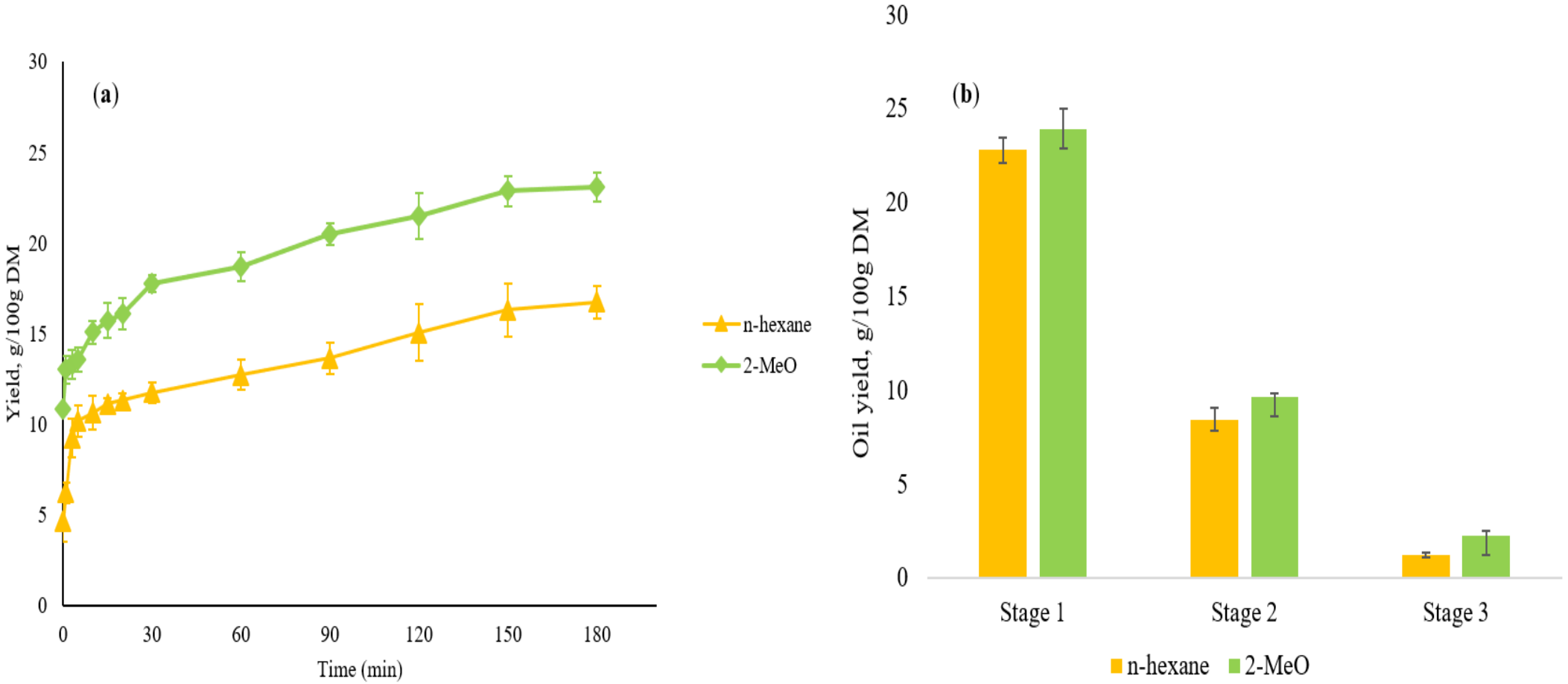
(a)
Yield, g/100g DM
Time (min)
0
30
60
90
120
150
180
5
10
15
20
25
n-hexane
2-MeO
(b)
Oil yield, g/100g DM
Stage 1
Stage 2
Stage 3
n-hexane
2-MeO

Figure 5.

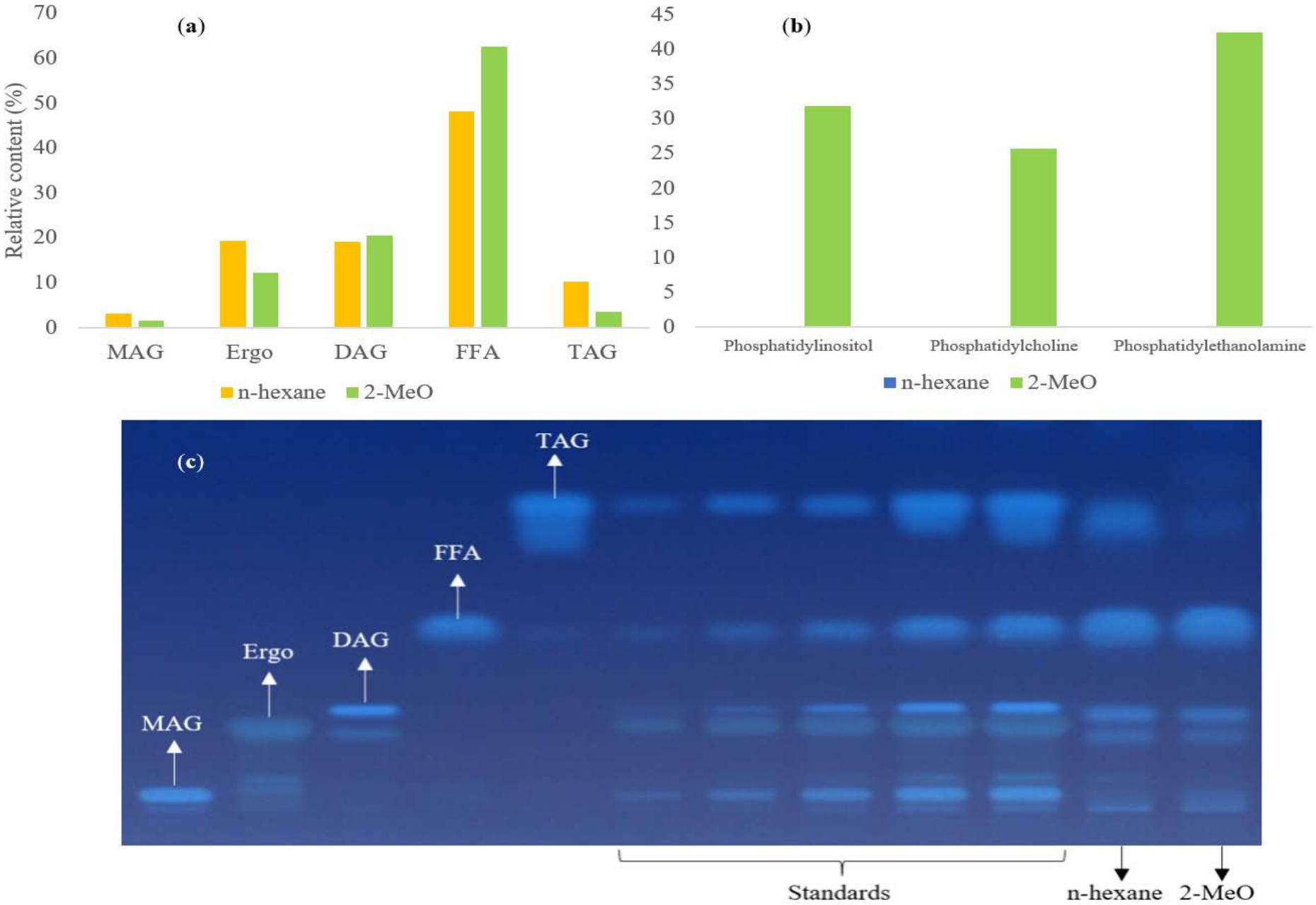
(a)
Relative content (%)
70
60
50
40
30
20
10
0
MAG
Ergo
DAG
FFA
TAG
n-hexane
2-MeO
(b)
45
40
35
30
25
20
15
10
5
0
Phosphatidylinositol
Phosphatidylcholine
Phosphatidylethanolamine
n-hexane
2-MeO
(c)
TAG
FFA
DAG
Ergo
MAG
Standards
n-hexane
2-MeO

Figure 6.

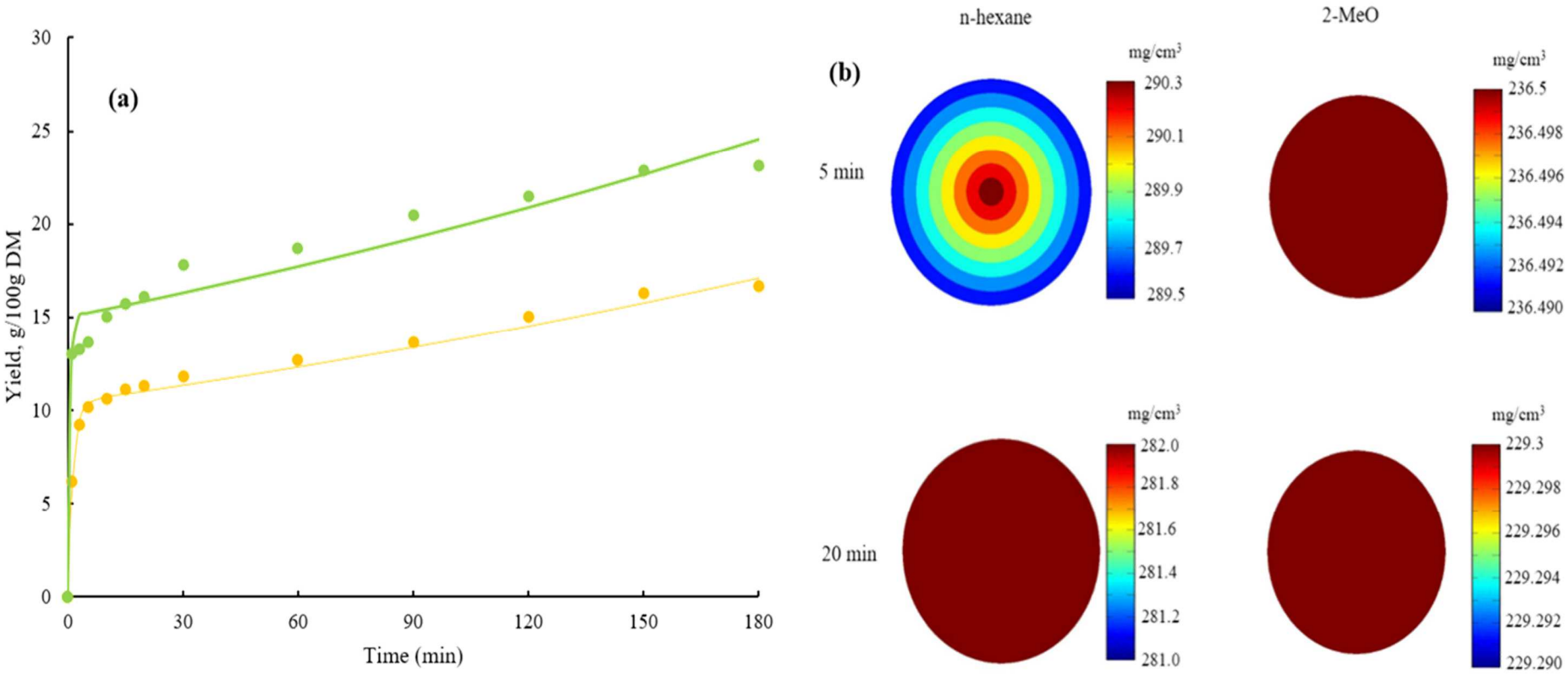
(a)
Yield, g/100g DM
Time (min)
0
5
10
15
20
25
30
0
30
60
90
120
150
180
(b)
n-hexane
2-MeO
5 min
20 min
mg/cm³
290.3
290.1
289.9
289.7
289.5
236.5
236.498
236.496
236.494
236.492
236.490
282.0
281.8
281.6
281.4
281.2
281.0
229.3
229.298
229.296
229.294
229.292
229.290

Figure 7.